

STUDY OF FRICTION AT NANO SCALE

Upendra Sharan Gupta¹, Shubham Jain², Devashish Dixit³, Harsh Jain⁴,
Sameer Singh Rathi⁵

^{1,2,3,4,5}Dept. of Mech. Engineering SVITS, Indore, (India)

ABSTRACT

In this paper, we are interested in the phenomenon of friction at the nanoscopic scale. we briefly review some macroscopic aspects to focus on the recent theories explaining the friction at the molecular level. We present our observed results on variation of friction as function of the AFM tip sliding velocities at different loads and humidity levels. The results explain the relation between the characteristics of the contacting surfaces and the different environment variables like the applied load or the humidity

Keywords: AFM tip, Microscopic Level, Relative humidity, Scanning Velocity, Tomlinson Model

I. INTRODUCTION

When two bodies contact each other and one of the bodies begins to slide against the other one, a force opposed to the movement appears. This force is called the friction force F_f . This aspect plays an important role in life. In some situations, the elimination of losses resulting from friction is desired, but in other situations, improvement of the friction is needed. Thus, the purpose of research in the field of friction is to understand its basic principles.

1.1 History of Friction

The first three laws should be summarized by the equation-

$$\mu = \frac{F_f}{F_n} = \text{Constant} \quad (1a)$$

That is friction force is directly proportional to normal force. Here the constant is independent of the area of contact and sliding velocity. so, there were some difficulties in explaining these laws. The contact surface of the bodies sliding the one against the other one is made of numerous asperities. It results that for the whole area of contact, the friction force corresponds to the sum over all the asperities. so for a single asperity junction

$$dF_{f,i} = dF_{n,i} \tan(\alpha_i) \quad (1b)$$

No adhesion is considered till now, so by time the model was completed for adhesive surfaces by adding a constant $F_{adh} = \mu \cdot F_o$

so that,

$$F_f = \mu \cdot (F_o + F_n) = F_{adh} + \mu F_n \quad (1c)$$

By this way, F_{adh} was the part of the friction force accounting for the intermolecular adhesive forces at the interface. Now they realised that these models are only able to explain static friction, they fail in explaining the dynamic friction. To overcome this problem, mechanisms of energy dissipation, grooving and

ploughing had to be included into the model. Now the friction force was written as $F_f = F_{adh} + F_{def} = \tau A + F_{def}$ (1d) F_{def} is ploughing, grooving or cracking of one surface by the asperities on other .

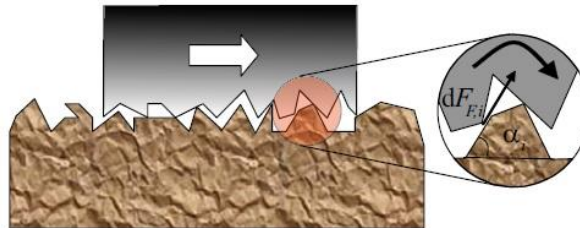


Figure 1: Schematic Representation of the Asperities at the Microscopic Scale .

II. THERMALLY ACTIVATED PHENOMENA IN NANOFRICTION

Behaviors of friction at macroscale are not valid at nanoscale all the time. The friction force presents numerous behaviors at the nanoscale when the sliding velocity is changed. Thus, the study of the friction phenomenon has to be done at scales relevant for its applications. we study the dependence of the nanofriction on the velocity, while taking into account the normal force and the humidity. The complete understanding of the velocity dependence of the friction at the nanoscale is still under current reflection. Since no real consensus has been found until now, we propose here a look back to the Tomlinson model and reviewed the main experimental results on the velocity dependence of the friction, having a look at the same time at the evolutions of the basic Tomlinson model to interpret the results. The two basic experimental observations about the friction phenomenon at the nanoscopic level are 1) The static and dynamic friction might be seen as two distinct frictional phenomena. The static force depends on the atomic structure of the sliding surfaces and the adhesion forces and can be related to the breaking of bonds. The dynamic friction is the force necessary to balance the energy losses due to the motion of one body against the other one. It is directly related to energy dissipation. 2) We observed a saw-tooth shape of the friction loop while scanning flat surfaces like mica. This shape is due to the atomic stick and slip of the tip sliding on the surface. It allows us to introduce the Tomlinson model explaining the experimental observations .

III. TOMLINSON MODEL

The Tomlinson model is a very simple and instructive mechanical model explaining already most of the phenomena occurring in friction, such as the atomic stick and slip, the static and the kinetic friction. In this model, the surface is described as a periodic arrangement of atoms whose potential of interaction with an AFM tip U_{ts} is usually approximated by a simple sine with a peak-to-peak amplitude U_0 and period a equal to the lattice periodicity.

$$U_{ts}(x) = -\frac{U_0}{2} \cos\left(\frac{2\pi x}{a}\right) \quad (1e)$$

Then, the system of the AFM tip attached to the cantilever is schematically represented by a point-like tip of mass m , usually an atom, attached to a spring of elastic constant k fixed to a support moving at the velocity v . The spring

is extended between the position of the tip (or atom) x and the position of the cantilever support $x_s = vt$, t being the time. The corresponding elastic potential, U_{el} , of the interaction between the tip and the support is then

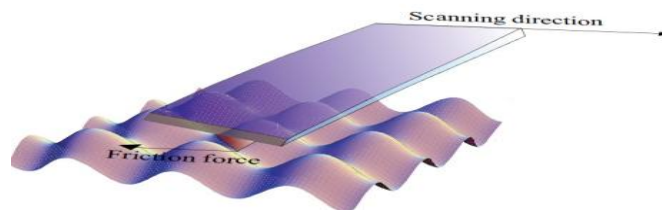


Figure . 2 Friction at Atomic Level, an AFM tip Slides Over an Atomically Flat Surface Represented by a Sinusoidal Potential of Interaction.

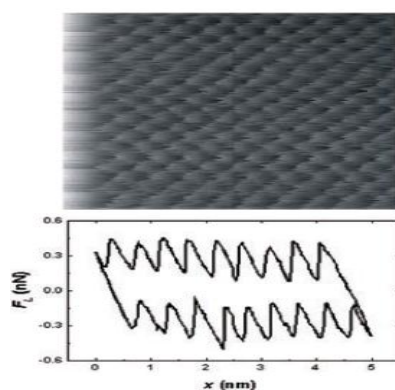


Figure 3 Friction Image and Loop

We clearly see the saw-tooth shape obtained for one loop over one line of scan.

$$U_{el} = \frac{k(x - x_s)^2}{2} \tag{1f}$$

The total energy of the system for a cantilever

$$U_{tot}(x, t) = -\frac{U_0}{2} \cos\left(\frac{2\pi x}{a}\right) + \frac{k(x - vt)^2}{2} \tag{1g}$$

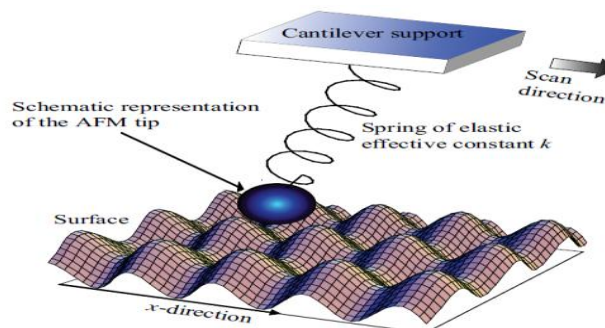


Figure . 4 Sketch of the Tomlinson Model.

A point-tip (the sphere) is attached through a spring to the cantilever support, which moves slowly along the x -direction. The tip slides on the surface and passes from one minimum to the next. As we see, the movement of the tip from one minimum to the next can be continuous or jumping depending on the relation between the corrugation U_0 and the elastic energy. Nevertheless, Tomlinson's model assumes that this change of position is done abruptly, meaning non adiabatically.

To be more general, it is possible to add to the equation of motion of the tip a damping term $\eta \dot{x}$ proportional to the tip velocity to account for energy dissipation. In this case, the motion of the tip over the surface is described by

$$m\ddot{x} - n\dot{x} = \frac{\pi U_0}{a} \sin\left(\frac{2\pi x}{a}\right) + k(x - vt) \tag{1h}$$

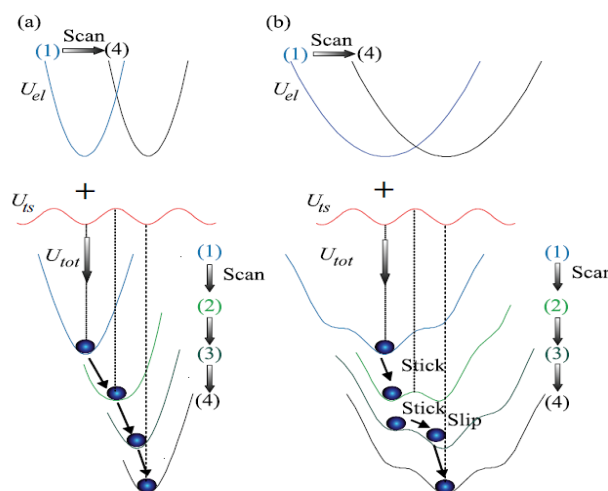


Figure . 5 Illustration of the Tomlinson model.

In this figure, the tip is schematically represented by the shaded circle always located at a minimum. (1)-(4) denote the time evolutions of the potential while scanning the surface. The total energy U_{tot} obtained by summing the elastic energy U_{el} stored in the spring with the tip-surface potential energy U_{ts} presents two cases: in (a), U_{tot} has only one minimum and the tip slides continuously over the surface. Such a case is peculiar to a stiff spring or cantilever. The sketch (b) illustrates the case of a soft cantilever. U_{tot} is characterized by several metastable minima whose result is a stick-slip behavior for the tip jumping from one minimum to the next.

It is possible to evaluate the critical lateral force $F_{F,c}$, that includes the jump from one minimum to other one

$$F_{f,c} = -k(x_c - vt) = \frac{k a}{2\pi} \sqrt{\frac{2\pi^2 U_0}{k a^2} - 1} \tag{1i}$$

In this model the static friction is given by

$$F_{f,stat} = \frac{\pi U_0}{a} \tag{1j}$$

The relation between the kinetic friction and the energy dissipated during the same period is

$$F_{f,kinetic} = \frac{\Delta W}{n a} \tag{1k}$$

Where n is an integer and ΔW is the energy dissipated during one period.

IV. RECENT EXPERIMENTAL RESULTS ON FRICTION AND EVOLUTION OF THE TOMLINSON MODEL

The Tomlinson model has served as basis for the interpretation of the experimental results on friction, notably for the understanding of the dependence of friction on the velocity. As we will see, the relation between friction

and scanning velocity has shown different and somewhat contradictory experimental results depending on the investigated surfaces and on the experimental conditions. To clarify the situation, we remind the most important results on velocity dependence of the friction and conclude by the two experimental studies that have shown the transition between a positive and a negative slope of the friction versus the velocity.

There were various setups and experiments organized by different authors at different time to observe the results on the relation between friction force and its dependence with the scanning velocity.

- 1) Independence of the friction versus the scanning velocity.
- 2) Logarithmic increase of the friction versus the scanning velocity.
- 3) Power-law increase of the friction versus the scanning velocity.
- 4) Logarithmic increase and decrease of the friction versus the scanning velocity.
- 5) Transition from a positive to a negative slope of the friction versus the velocity.

To conclude this section, two main behaviors emerge from the review of the experimental results.

1) Thermal activation involving vibrations that may excite the slipping from one equilibrium position to the next one. For this kind of thermal activation, the increase of the velocity reduces the probability of transition between the different equilibrium positions and thus it leads to a logarithmic increase of the friction with the sliding velocity.

2) We have time dependent processes involving intermolecular forces and leading to a logarithmic decrease of the friction force with the scanning velocity. It can be thermal activation of water bridges between the AFM tip and the surface, but also layers covering the surface and whose disorganization under the applied shear stress results in a decrease of the friction force once they do not have enough time

V. PRESENTATION OF OUR THEORETICAL MODEL

We present the theoretical developments related to the phenomenological models used to describe the experimental results. The friction measurements have been performed in an environment where the temperature was almost constant ($T \sim 24^\circ$) and the humidity continuously controlled. By this way, it has been possible to highlight thermally activated processes, and more precisely the balance between the activation of capillary bridges and thermal vibrations. For this purpose, we will show the transition from the hydrophilic to the hydrophobic regime of the friction, by scanning with the same AFM tip a single area of a CrN surface. The linear dependence of the friction on the logarithm of the sliding velocity for both hydrophobic and hydrophilic surfaces has already been explained. Until now, two different models were commonly used to explain either the increasing or the decreasing friction as function of the sliding velocity. Here we present a theoretical model including both, the increase and decrease of FF with $\ln v$. A special behavior related to hydrophobic surfaces was the observation of apparent plateaux at sufficiently high sliding velocities for the curves of friction versus the logarithm of the sliding velocity. Our experimental results reveal also a similar behavior for hydrophilic surfaces and is explained in our model by the analytical relationships between the humidity, the velocity and the normal load.

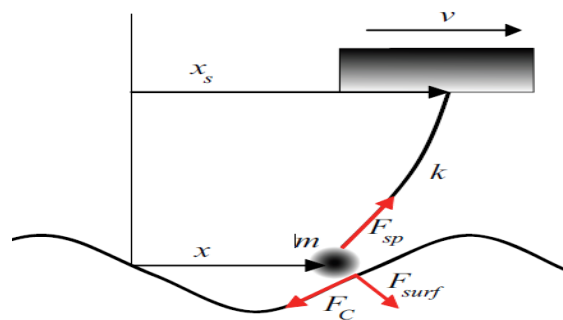


Figure . 6 Sketch of a point-tip of mass m and coordinate x connected via a spring of constant stiffness k to a support moving at a constant velocity v . The point-tip moves in a corrugated substrate potential undergoing capillary forces F_C , surface forces F_{surf} and the spring force

F_{sp}

VI. THEORETICAL MODEL

Our theoretical model is based on recent developments of the relationships between the friction force F_F and the dynamic energy barrier ΔE which separates two stable positions of the AFM tip relative to the surface. It can be described as a modified Tomlinson model, taking into account the effects of capillary forces and thermal activation. Considering the sliding system shown in Fig.5. An AFM tip represented by a point-object of mass m moves on a surface and experiences the corrugated sinusoidal potential of interaction due to the tip-surface forces F_{surf} . The tip is coupled to a cantilever support by a spring of effective elastic constant k [N/m]. This effective spring constant is experimentally deduced from the slope of the friction force versus distance curves performed on the studied sample. The cantilever support is moving at a velocity $v = \text{constant}$ and with its position described by $x_s = vt$. We take into account the thermally activated condensation of liquid bridges by introducing the capillary force F_C . This force is opposed to the tip displacement and its effect results in a non symmetric surface-tip energy barrier as illustrated in Fig.6. From a simple point of view, the equation of motion is then given by

$$m\ddot{x} = F_{sp} + F_{surf} + F_C = k(vt - x) - U'(x) - F_C \quad (11)$$

where x is the position of the tip and t the time.

$U'(x) = dU(x)/dx$ is the first derivative of the corrugated substrate potential $U(x)$ experienced by the point-tip with respect to x , and F_{sp} is the conservative force resulting from the spring. We will not take into consideration other couplings of the point-tip to the sample surface. We consider now a line of motion along the x -axis and in the direction of $x > 0$, representing for example the movement of the AFM tip from a starting point $x = A$ to a position $x > A$ during a scanning process. Whereas F_{sp} and F_{surf} are conservative forces F_C that derive from a potential U^c following the relation $F_C = -\text{grad}(U^c)$, F_C is a non conservative force F_{nc} that is always opposed to the tip displacement. Thus, the potentials related to the conservative forces only depend on the starting and ending point of the line of motion, whereas the work done by F_C depends on the route along which the force acts. In our case, this route is a straight line going from the starting point A to some position x with $x > A$. Then, in the case of a sinusoidal surface potential $U(x)$, the energy describing the combined surface-tip-cantilever system can be approximated by

$$E(X, t) = \frac{1}{2}k(vt - X)^2 - \frac{E_0}{2} \cos\left(\frac{2\pi X}{a}\right) + Fc(X - X_c) \quad (1m)$$

where x_c is a parameter related to a mean position of the bases of the capillary bridges on the static surface. E_0 is half the surface barrier potential, a is the lattice constant of the sample surface.

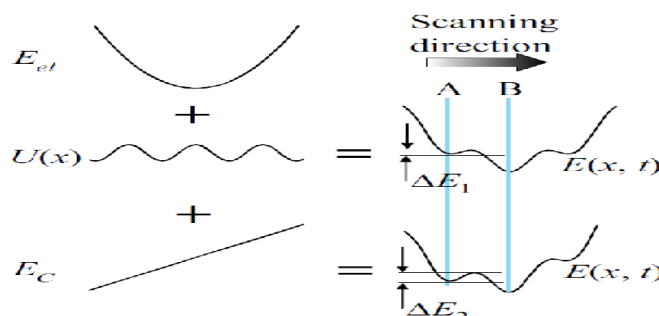


Figure .7 Effect of the capillary force on the total balance of energy $E_{x,t}$ of the system. E_{el} is related to the spring energy, $U(x)$ is the tip-surface corrugated energy and E_c is an approximation of the energy related to the capillary bridges meaning that it costs some energy to move in the sliding direction due to the presence of the capillary bridges. Without the capillary force, $E_{x,t}$ has a symmetric shape, whereas adding the energy E_c breaks the symmetry resulting in the increase of the energy barrier ΔE needed to go from A to B, such that $\Delta E_1 < \Delta E_2$. For critical positions of the support, the AFM tip will overcome the energy barrier $\Delta E(t)$ between two consecutive extrema $E_{min}(x, t)$ and $E_{max}(x, t)$. The critical position is given by (i) $\partial E(x^*, t^*)/\partial x = 0$ and (ii) $\partial^2 E(x^*, t^*)/\partial x^2 = 0$, where x^* and t^* are respectively the critical position and the critical time for which the potential barrier vanishes.

By taking $x_2 > x_1$, we finally obtain for the energy barrier:

$$\left. \frac{\partial E(x, t)}{\partial x} \right|_{x=\frac{a}{4}} = 0 \Leftrightarrow x_{1,2} = \frac{1}{4} \left(a \pm \frac{2\sqrt{2}}{E_0\pi^{3/2}} \sqrt{a^2 E_0 (E_0\pi - aktv)} \right) \quad (1n)$$

$$\Delta E(t) = E_{max}(x, t) - E_{min}(x, t) = E(x_2, t) - E(x_1, t)$$

With $F^* = \pi E_0/a$

In more general, we have

$$\Delta E(Ff) = \frac{1}{\beta} \left(1 + \frac{Fc}{F^*} - \frac{Ff}{F^*} \right)^{3/2} \quad (1o)$$

where β and F^* depend on the shape of the interaction potential between the tip and the surface. At zero temperature $T = 0$, the tip will move from a stable position to the following one when $\Delta E = 0$, leading to $F_f = F^*$. This result may explain the independence of the friction on the velocity in some works where thermal activation was not supposed. In the case of finite temperatures T , $\Delta E(t)$ is comparable to kBT , kB being the Boltzmann constant. Then, the master equation describing the probability $p(t)$ that the tip does not jump over the energy barrier takes the form

$$\frac{dp(t)}{pt} = -f_0 \exp\left(-\frac{\Delta E(t)}{KbT}\right) p(t) \quad (1p)$$

Where f_0 is a characteristic attempt frequency of the system. The probability of jumping due to the thermal activation has its maximum at $d^2p/dt^2 = 0$. In our case, we are interested in the friction force maximizing the probability for overcoming the energy barrier. We have to exchange the temporal variable t by F_f , so that

$$\frac{d^2p(F_f)}{dF_f^2} = 0$$

Which leads to

$$\ln\left(\frac{2F_0\beta K b T F^*}{3k v}\right) - \frac{1}{2}\ln\left(1 + \frac{F_c}{F^*} - \frac{F_f}{F^*}\right) = \frac{1}{\beta K b T} \left(1 + \frac{F_c}{F^*} - \frac{F_f}{F^*}\right)^{\frac{3}{2}}$$

We finally obtain the mean lateral force F_f :

$$F_f = F^* + A \ln \frac{v_0}{v} - \left[\frac{\beta K b T}{3} W \left(\frac{3(F^* v^2)^{\frac{3}{2}}}{\beta K b T v^3} \right) \right]^{\frac{2}{3}} \quad (1q)$$

$$= F^* + F_C - F_{SS}$$

From this equation, F_C decreases with increasing the scanning velocity, whereas $F_{SS}(\ln v)$ increases. From the order of magnitude one observes that $F_C \gg F_{SS}$ for sufficiently high humidity. Then by reducing the relative humidity, the capillary force decreases progressively to become of the order of F_{SS} . The result is a competition between F_C , which adds to F^* , and F_{SS} , which is subtracted from F^* . From the competition between F_C and F_{SS} results the shape of the friction curve versus the natural logarithm of the scanning velocity: a positive slope for low humidity and negative slope for high humidity.

With

$$v_1 = \frac{2f_0\beta K b T}{3k\sqrt{F^*}}$$

This last equation describes the phenomenology of F_C in terms of capillary bridges between the asperities of the tip and the surface. v_0 is a characteristic velocity of the system "tip - capillary bridges - surface". W is the lambert-W function defined as $W(x) \exp(W(x)) = x$. v_1 has the meaning of an upper velocity limit defined for the increasing sliding friction versus $\ln v$.

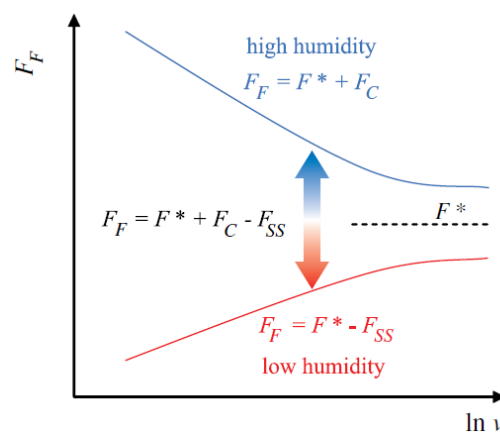


Figure .8 Illustration of the behavior of F_F versus $\ln v$.

The transition from a positive to a negative slope of F_F vs. $\ln v$ is explained in terms of competition between F_C and F_{SS} . The action of F_C dominates at high humidity, but becomes negligible as the humidity decreases, which gives rise to the slope transition.

VII. CONCLUSION

In this paper, we were interested in the friction phenomenon, an old subject of research that still remains topical due to its application in industry and everyday life. One of the important changes occurring in the field of the friction research has been the scale reduction of the studies, going from the macroscopic world to the atomic level. At these small scales, the balance between forces proportional to the surface and the volume is not the same as the one for macroscopic bulk material. The result is a divergence of the phenomenological behaviors depending on the size of the system. To enlarge our knowledge on the friction at the nanometer scale, we studied the changes in the friction force for a nanoscopic AFM tip sliding on various samples, while exterior parameters, such as the scanning velocity, the applied normal load or the humidity varied. Emphasis was carried on the thermally activated phenomena occurring in the nanoscopic friction by the investigation of the friction dependence on the velocity. The main experimental results were the logarithmic dependence of the friction on both the scanning velocity and the relative humidity. For the first time, a transition from a positive to a negative slope of the friction force versus the logarithm of the sliding velocity has been observed for the very same tip-surface contact, by varying the relative humidity. The complexity of the friction phenomenon results in the difficulty of finding a fundamental model to explain its different behaviors. This complexity emerges from its universal nature, meaning the great variety of materials that are in relative motion the one against the other one. If an analytical comprehension of the frictional process is not possible, other apertures are given by the computer sciences. It is now possible to simulate the interactions between contacting bodies at the molecular level. Perhaps a complete comprehension of the friction is not yet possible, but in the actual climate of economy of energy, whatever could reduce the friction becomes relevant and might have non negligible consequences.

REFERENCES

- [1] B. Derjaguin, *Kolloid-Zeits.* 69, 155 (1934).
- [2] B. Bhushan, *Handbook of Micro/NanoTribology* (CRC Press, 2nd Ed., 1999).
- [3] J. Gao, W. D. Luedtke, D. Gourdon, M. Ruths, J. N. Israelachvili, and U. Landman, *J.Phys. Chem. B* 108, 3410 (2004).
- [4] F. P. Bowden and D. Tabor, *Brit. J. Appl. Phys.* 17, 1524 (1966).
- [5] J. A. Greenwood, *Fundamentals of friction* (Kluwer: Dordrecht, 1992).
- [6] B. Persson, *Sliding Friction: Physical Principles and Applications* (Springer: Berlin, 2000).
- [7] A. Socoliuc, R. Bennewitz, E. Gnecco, and E. Meyer, *Phys. Rev. Lett.* 92, 134301 (2004).
- [8] E. Gnecco, R. Bennewitz, T. Gyalog, C. Loppacher, M. Bammerlin, E. Meyer, and H.-J. Güntherodt, *Phys. Rev. Lett.* 84, 1172 (2000).
- [9] G. A. Tomlinson, *Philos. Mag.* 7, 905 (1929).
- [10] M. Hirano, *Surf. Sci. Rep.* 60, 159 (2006).
- [11] C. Fusco and A. Fasolino, *Phys. Rev. B* 71, 045413 (2005).

- [12] N. Sasaki, M. Kobayashi, and M. Tsukada, Phys. Rev. B 54, 2138 (1996).
- [13] C. M. Mate, G.M.McClelland, R. Erlandsson, and S. Chiang, Phys. Rev. Lett. 59, 1942 (1987).
- [14] O. Zwörner, H. Hölscher, U. D. Schwarz, and R. Wiesendanger, Appl. Phys. A 66, 263(1998).
- [15] T. Bouhacina, J. P. Aimé, S. Gauthier, D. Michel, and V. Heroguez, Phys. Rev. B 56,7694 (1997).
- [16] E. Riedo and E. Gnecco, Nanotech. 15, S288 (2004).
- [17] E. Riedo, I. Palaci, C. Boragno, and H. Brune, J. Phys. Chem. B 108, 5324 (2004).
- [18] J. Chen, I. Ratera, J. Y. Park, and M. Salmeron, Phys. Rev. Lett. 96, 2361021 (2006).
- [19] P. Reimann and M. Evstigneev, New J. of Phys. 7, 25 (2005).
- [20] M. A. Lantz, S. J. O'Shea, M. E. Welland, and K. L. Johnson, Phys. Rev. B 55, 10776,(1997).